

Original Research

The Durability of Reinforced Concrete Structures with 35 Years of Service in Offshore Environment

Dejun Fu*

Ningbo City College of Vocational Technology, Ningbo 315000, China

Received: 28 April 2023

Accepted: 26 August 2023

Abstract

Durability plays a crucial role in maintaining the service life of a structure. This paper focuses on examining the durability of a building with a reinforced concrete structure that has been exposed to an offshore environment for 35 years. The study involved on-site inspections to assess external damage, including testing parameters such as the compressive strength of the concrete material and the overall tilt of the building. Additionally, microscopic inspection techniques, such as X-ray fluorescence (XRF), thermogravimetry-differential scanning calorimetry (TG-DSC), X-ray diffraction (XRD), and scanning electron microscopy (SEM), were employed to analyze the corrosion products and microstructure associated with the damage mechanism. Based on the data obtained from the on-site inspections, structural calculation software was used to calculate and verify the overall load-bearing capacity of the building, aiming to determine its safety level. The evaluation results revealed severe safety issues within the building, despite it not having reached its designed service life, particularly in relation to reinforcement corrosion.

Keywords: offshore environment, reinforced concrete structures, durability, field inspection tests, service life

Introduction

Buildings located in poor service environments are susceptible to corrosive media, moisture, high temperatures, heavy loads, and improper maintenance, among other factors. Over time, these conditions can undermine or even disable the durability and functionality of the buildings before their intended design life. Such deterioration directly impacts the normal order of life and work, as well as the safety

of individuals and property, leading to significant economic losses and social consequences [1-5].

For buildings with reinforced concrete structures, the deterioration of their durability can be classified into two types: one resulting from the corrosion and degradation of the concrete materials themselves [6-8], and the other from the corrosion of reinforcement bars within the concrete [9-11]. Numerous examples have demonstrated that the latter factor significantly contributes to the deterioration or failure of reinforced concrete.

The corrosion of reinforcement bars inside the concrete is primarily caused by concrete carbonization and the erosion of chloride ions. Carbon

*e-mail: 376211608@qq.com

dioxide (CO_2) in the atmosphere reacts with calcium hydroxide ($\text{Ca}(\text{OH})_2$) in the concrete, forming calcium carbonate (CaCO_3), which reduces the alkalinity of the concrete. When the pH value reaches or falls below 9, the passivating films on the reinforcement bars become unstable, and the bars, without the protection of these films, start corroding under certain environmental conditions [12-15]. Additionally, even at low concentrations, chloride ions can significantly destroy the passivating films on the reinforcement bars, further promoting corrosion under specific conditions [16].

While carbon dioxide constitutes a small proportion of the natural atmosphere (only about 0.03%), and the carbonization rate of concrete is relatively slow in the natural environment, over a long period (e.g., several decades), reinforcement bars are susceptible to carbonization and subsequent corrosion after the passivating films are destroyed. The natural environment contains various sources of chloride ions, such as oceans, offshore areas, inland salt lakes, and chemical industries that produce corrosive media like hydrochloric acid and chlorine [17-20]. Experimental results indicate that chloride ions diffuse into concrete at a faster rate than the rate of concrete carbonization, making substances with chloride ions significantly contribute to the prevalence and severity of reinforcement bar corrosion in concrete [21].

Furthermore, studies have shown that the combined effects of carbonation and chloride ions are greater than the effects of each factor considered individually [22, 23]. Carbonation has a profound influence on the transport of chloride ions within building structures. Specifically, carbonation significantly increases both the diffusion rate and content of chloride ions, which detrimentally affect the working life of structures [21]. Carbonation can release bound chloride ions, turning them into free ions. The chloride ion content in carbonated concrete is significantly higher than that in non-carbonated concrete, and carbonation even facilitates the migration of chloride ions [24].

Special attention should be given to the poor durability performance of reinforced concrete structures in offshore areas, as highlighted by numerous scholars [25]. For instance, in a power station's booster station that has been in service for 26 years, 70% of the concrete columns and 25% of the concrete beams exhibit severe durability damages, such as longitudinal cracks and exposed bars. Moreover, concrete members in the tidal range zone of a wharf that directly interacts with seawater suffer extensive corrosion from chloride ions. Investigations indicate that wharves in service for 20 to 30 years generally exhibit serious durability problems.

This paper focuses on a reinforced concrete house in an offshore area that has been in service for 35 years. Through on-site investigations, assessment of the house's condition, analysis of visible damages, and examination of the compressive strength of load-bearing concrete beams and columns, the damage mechanism of concrete materials and internal reinforcement bars is scrutinized

using microscopic inspection methods. Finally, with the assistance of relevant structural calculation software, the overall safety and safety grade of the house's current state are calculated and analyzed. Conclusions are drawn, and appropriate recommendations are proposed.

Material and Methods

An Overview of the House and Detection Methods

Location of the House and the Climate

The house is situated approximately 3 kilometers away from the sea, as illustrated in Fig. 1. The region falls within the subtropical monsoon climate zone, known for its mild and humid climate, distinct four seasons, abundant sunshine, and rainfall. The average annual temperature in the area is 16.3°C , and the annual precipitation ranges from 1310 to 1370 mm. On average, there are 148 rainy days throughout the year. Typhoons commonly occur during the summer and autumn seasons. Spring is characterized by lower temperatures and increased rainfall, while cloudiness and rain are prevalent features of the autumn season.

An Overview of the Architectural Design of the House

The house is a six-story reinforced concrete structure (partially eight stories). It faces north-south, whose plan shape is rectangular, and the main axis size is $75.30\text{ m} \times 13.80\text{ m}$. The total floor area of the structure is about 6200 m^2 , and it is 30.70 m in height. The house was built in the mid-1980s. Fig. 2 is the south elevation of the inspected house, and Fig. 3 is the first-floor plan of the house.

The house adopts a pile foundation composed of 250 precast concrete square piles that are 23 m in length. The design value of the concrete strength is 38 MPa , and the piles are connected with steel-capped sulfuric

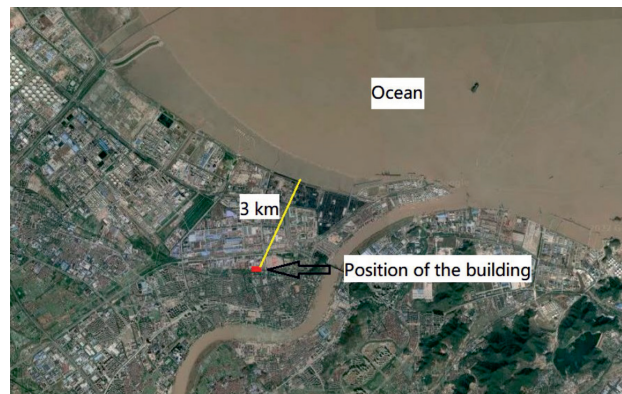


Fig. 1. Location of the building.

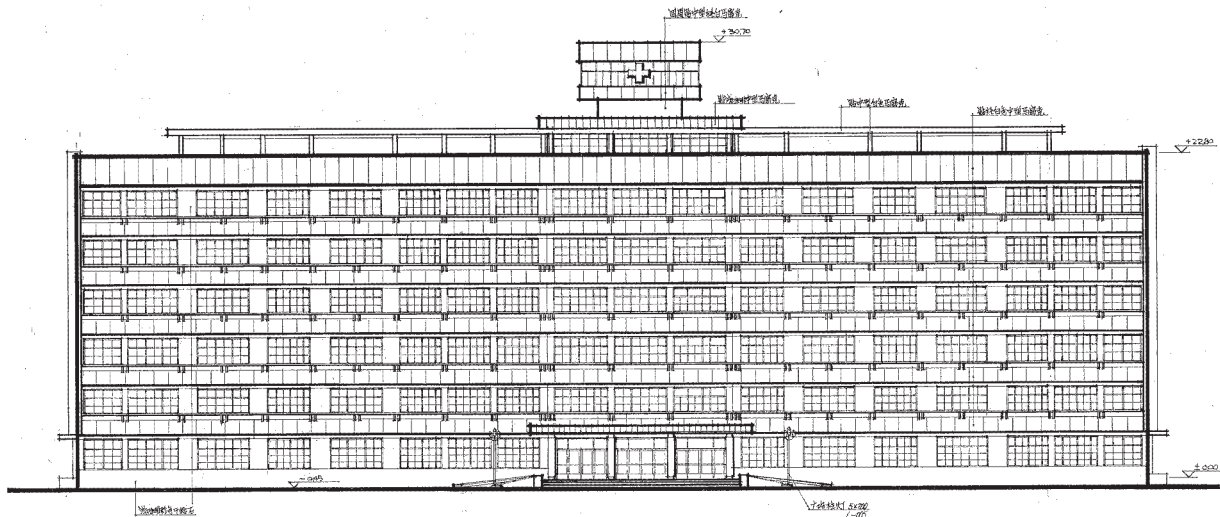


Fig. 2. South elevation of the building.

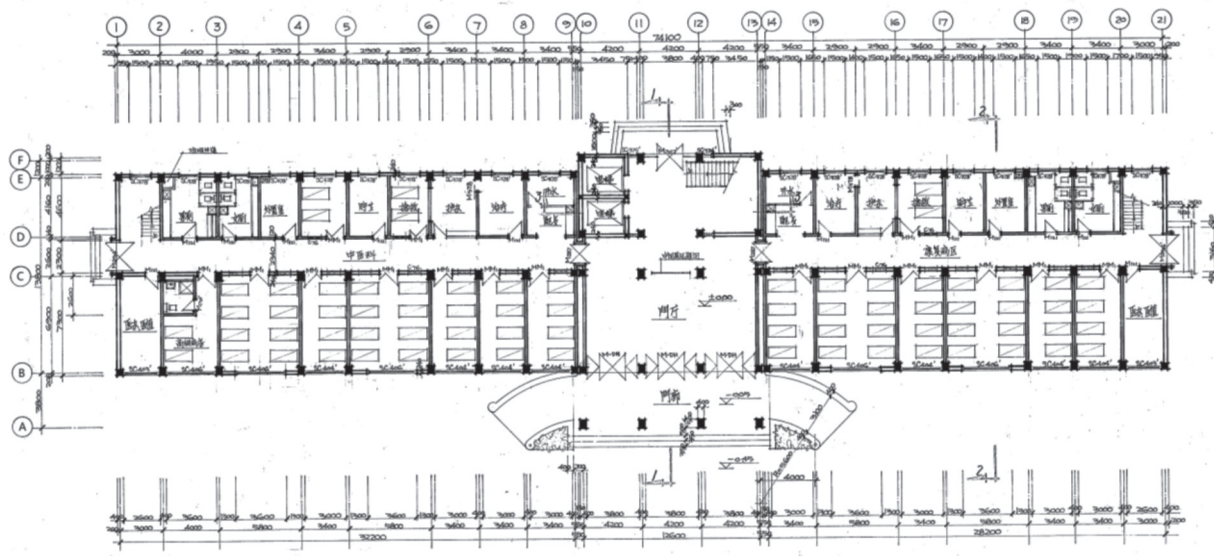


Fig. 3. Ground floor plan of the building.

cement. The design values for the strength of the foundation cap, concrete beams, and other parts are 18 MPa, and that of the concrete materials at the bottom of the main structures is 23 MPa. The stair slabs and the stair beams are made of cast-in-place concrete; the reinforcement bars are of HPB235 and HRB335 types; their diameters are mainly 18 mm, 20 mm, 22 mm, and 25 mm. The thickness of the floor slab is generally 80 mm and 100 mm. The water tank at the top of the house is made of compact concrete and HPB235-type reinforcement bars. The concrete is poured at one time, leaving no construction joints.

Concrete beams and columns buttress the upper part of the house. The main dimensions of the concrete columns are 250 mm×250 mm, 400 mm×400 mm, 400 mm×500 mm; the main dimensions of the concrete beams are: 150 mm×440 mm, 200 mm×400 mm,

200 mm×720 mm, 200 mm×970 mm, 250 mm×680 mm, 250 mm×720 mm, 250 mm×930 mm. The floor and roof panels are mainly the prestressed concrete perforated slabs, and the slabs in the six stories and some areas (located in the axes of 2-4×D-E, 5-6×D-E, 8-9×D-E, 14-16×D-E, 17-20×D-E, among others) are cast-in-place concrete slabs. The roof adopts SBS waterproof membrane and the three stairs in the house are made of cast-in-place reinforced concrete.

Detection Methods

Macro Detection Methods

(1) Appearance inspection: The inspectors were used to observe the whole house with the naked eye. The surface stucco layer was removed, if necessary,

to observe the internal damage. Photos of the existing problems were taken.

(2) Test of the compressive strength of concrete: ZC3-A concrete rebound tester was used to test the strength of the concrete structural members of the house. Specifically, the concrete surface stucco layers of the inspected members were chipped away until the solid surface was exposed; after handling the surface of the members with a grinding wheel, the rebound value and the carbonization depth were measured with a rebound tester and a carbonization depth gauge, respectively; with the corrected value of rebound angle and the average carbonation depth, the concrete strength of each measured area was calculated, based on which the compressive strength of each member was calculated [26].

(3) Measurement of the overall inclination of the house: According to JGJ 8-2016, the J2-2 theodolite and a steel ruler with a range of 30 mm were used on site to measure the verticality of the walls, in accordance with relevant regulations of the theodolite surveying in deformation measurement [27].

Micro Detection Methods

(1) X-ray fluorescence (XRF)

The X-ray fluorescence spectrometer of ARLADVNT3600 was utilized to detect and analyze the chemical composition of concrete powder, as well as its element content.

(2) Simultaneous thermal analysis (STA)

With a German synchronous thermal analyzer (NETZSCH, STA449F3Jupiter), the thermal properties of concrete powder samples were detected and analyzed with the methods of thermogravimetric (TG) and differential scanning calorimetry (DSC) analysis. The detection was conducted in a nitrogen atmosphere, with the temperature ranging from room temperature to 900°C, the heating rate being 20°C/min.

(3) X-ray diffraction (XRD)

The chemical composition of concrete materials was detected and analyzed with a BRUKER DB Advance X-ray diffractometer. With the electrical voltage and current at 40 kV and 40 mA respectively, Cu K α radiation, $\lambda = 1.5406\text{\AA}$, was diffracted from 7.5° to 42.5°, with a step size of 0.02° and a scan time of 0.1 s/step. Subsequently, a quantitative analysis of XRD measurement results was conducted to figure out the chemical composition using the method of Rietveld.

(4) Scanning electron microscope (SEM)

Regulus 8100 SEM, made by HITACHI, Japan, was used to carry out the test with the electrical voltage at 20 kV. The built-in energy dispersive X-ray spectrometer was utilized to analyze the composition of elements in designated areas.

Results and Discussion

Detection Results and Check on Structural Safety

Appearance Inspection Results

Foundation

The on-site inspection results showed that there supervened no obvious cracking of the superstructure due to differential settlement.

Superstructure

(1) Concrete members: The house is a frame structure with concrete beams and columns as the main load-bearing members. On-site inspection results demonstrated that the concrete protective layers burst and peeled off, and reinforcement bars corroded in several sites inside the house, i.e., the 2×C-E beam, 2×E column and ladder beams on the first to third floors of the west staircase, and 20×C-E beam, 20×E column on the first to fourth floors of the east staircase. Details are shown in Fig. 4. Except for part of the overhanging eaves of the north facade whose concrete was peeled off and reinforced concrete corroded, the rest of the load-bearing members were in normal service.

(2) Floor and roof panels: water seepage occurred on 1st floor 7-8×B-C, 3rd floor 19-20×B-C and 5th floor 19-21×B-C floor panels, computer room, and roof panels of the west staircase.

(3) Walls: water seepage and stucco layers peeling off were serious on the wall axes of 1st floor 1×B-C, 14-15×E, 21×D-E, 3rd floor 21×B-C, 4th floor 1×B-C, and 5th floor 1×E.

Envelop Enclosure and Others

Water seepage occurred at the expansion joints and the roof waterproofing membranes were aging.

Detection Results of Strength and Overall Inclination of Concrete Materials

Detection Results of Strength

A total of 25 concrete beams and columns were randomly selected. The results showed that the age-corrected value of concrete strength was between 19.3 and 29.2 MPa, the average value of concrete strength was 23.5 MPa, and its standard value was 18.6 MPa which was slightly different from the design value. The carbonization depth of all members was greater than 6mm, and more details are shown in Table 1.

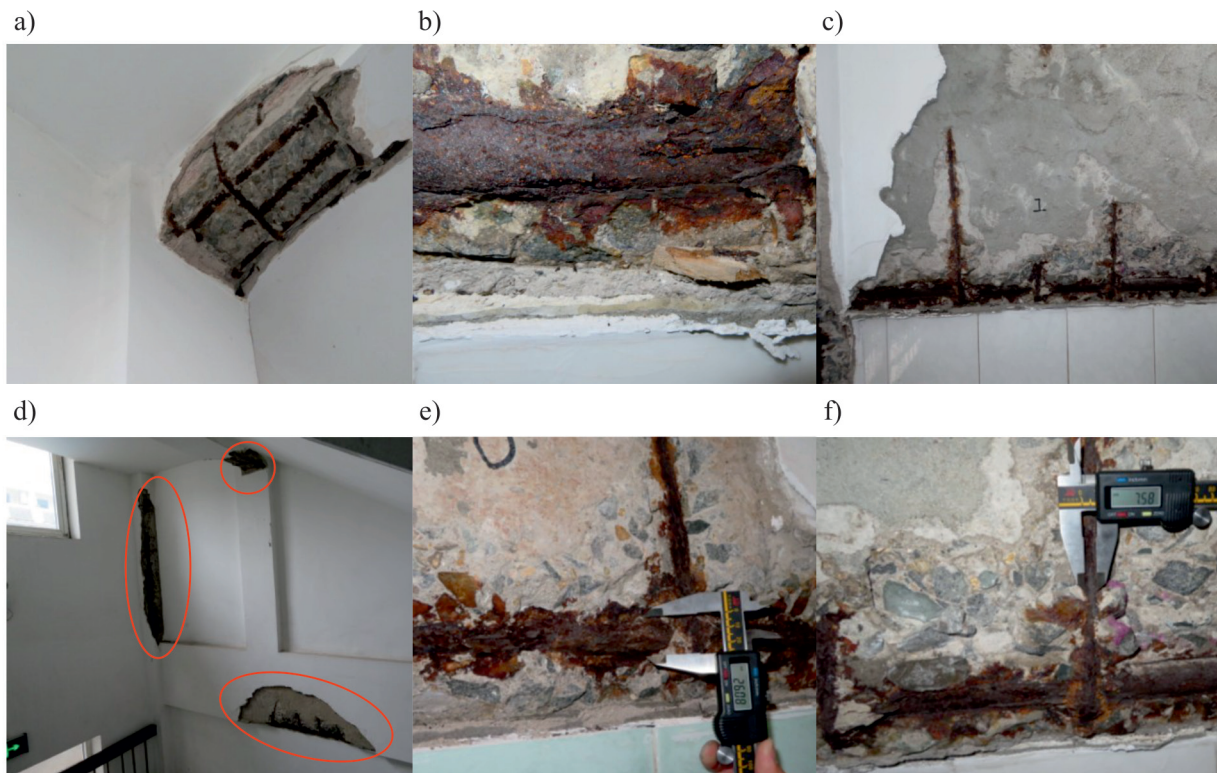


Fig. 4. Various conditions of steel corrosion: a) Corrosion of steel bars in the beam as a whole; b) local corrosion of steel bars; c) corrosion of longitudinal bars and stirrups in beams; d) corrosion of steel bars in beams and columns; e) diameter of longitudinal bars after corrosion; and f) diameter of stirrups corroded.

Detection Results of Inclination

Due to the limitations of the on-site environment, two observation points were set and a total of 4 inclination values were obtained. The inclination from the observation points was 0.3‰ and 1.0‰, which were within the normal range and accorded with the designated limit value specified in Article 7.3.10 of GB 50292-2015 [28]. Detection results are displayed in Table 2.

Micro Detection Results

X-ray fluorescence spectrometer was used to analyze the concrete powder samples, and the chemical elements and oxide composition content were obtained. According to the results, the chemical elements are mainly Calcium (Ca), Silicon (Si), Aluminium (Al), Ferrum (Fe), and others, whose content are similar to those of ordinary concrete. However, it's worth noting that the Chlorine (Cl) content was up to 1.47%, far more than the 0.06% limit designated in GB 50010-2010 (2015 edition) [29]. Tables 3 and 4 provide more details. The high chlorine content of the concrete may be attributed to the use of sea sand or the close location of the house to the sea.

According to the results of the simultaneous thermal analysis (STA) of concrete powder, the trough

around a temperature of 100°C signaled the heat loss caused by water evaporation inside the concrete, which corresponded to the process of products of cement hydration removing free water. An endothermic peak around 680°C represented the decomposition of CaCO_3 , and the mass loss embodied the release of CO_2 . No obvious trough in the TG-DSC curve around 430°C meant no Ca(OH)_2 in the concrete. Detailed results are shown in Fig. 5.

The results gained through XRD analysis also supported the above argument that no Ca(OH)_2 existed in the concrete. Ca(OH)_2 in the concrete was carbonized into CaCO_3 after over 30 years. XRD results in Fig. 6a) illustrated that the chemical composition of concrete materials was mainly SiO_2 and CaCO_3 , and results in Fig. 6b) demonstrated that the main composition of the corroded reinforced concrete powder was rust.

A micro detection of the appearance of concrete samples was conducted with a scanning electron microscope and it's discovered that there were many micro-cracks and holes on the surface of the concrete samples, and the concrete was partially loose, which may affect the strength of the concrete. Moreover, besides C-S-H gel elements, such as Ca, Si and O, other elements like Al, C, Mg, S, Cl were also discovered in the local area of the concrete samples by virtue of energy spectrometer. The results are shown in Fig. 7.

Table 1. Test results of compressive strength of concrete members.

Serial Number	Component name	Carbonation depth (mm)	Average value (MPa)	Standard deviation (MPa)	Estimated strength of concrete (MPa)	age-corrected value (MPa)
1	1 st floor 1 x E column	6.0	34.9	1.9	31.7	28.2
2	1 st floor 11×D column	6.0	31.0	1.3	28.9	25.7
3	1 st floor 21×E column	6.0	33.2	2.3	29.4	26.2
4	1 st floor 2×C-E beam	6.0	31.4	1.4	29.1	25.9
5	1 st floor 11-12×D beam	6.0	33.1	1.7	30.4	27.1
6	1 st floor 20×C-E beam	6.0	25.9	1.6	23.3	20.7
7	2 nd Floor 1×E column	6.0	28.8	1.0	27.1	24.1
8	2 nd Floor 11×F column	6.0	28.1	1.7	25.3	22.5
9	2 nd Floor 21×E column	6.0	26.1	1.5	23.6	21.0
10	2 nd Floor 2×C-E beam	6.0	36.6	2.3	32.8	29.2
11	2 nd Floor 20×C-E beam	6.0	27.0	0.5	26.2	23.3
12	3 rd Floor 1×E column	6.0	29.6	1.2	27.6	24.6
13	3 rd Floor 12×F column	6.0	23.8	1.3	21.7	19.3
14	3 rd Floor 21×E column	6.0	26.2	1.5	23.7	21.1
15	3 rd Floor 2×C-E beam	6.0	28.2	1.1	26.3	23.4
16	3 rd Floor 20×C-E beam	6.0	25.4	1.8	22.4	19.9
17	4 th Floor 1×E column	6.0	28.8	2.1	25.3	22.5
18	4 th Floor 21×E column	6.0	23.6	1.2	21.7	19.3
19	4 th Floor 2×C-E beam	6.0	29.6	1.8	26.7	23.8
20	4 th Floor 20×C-E beam	6.0	28.7	1.3	26.5	23.6
21	5 th Floor 1×E column	6.0	26.8	0.8	25.5	22.7
22	5 th Floor 21×E column	6.0	28.1	1.2	26.1	23.2
23	5 th Floor 2×C-E beam	6.0	26.8	0.9	25.4	22.6
24	5 th Floor 20×C-E beam	6.0	29.2	1.3	27.0	24.0
25	7 th Floor 12×D column	6.0	27.4	0.5	26.6	23.7

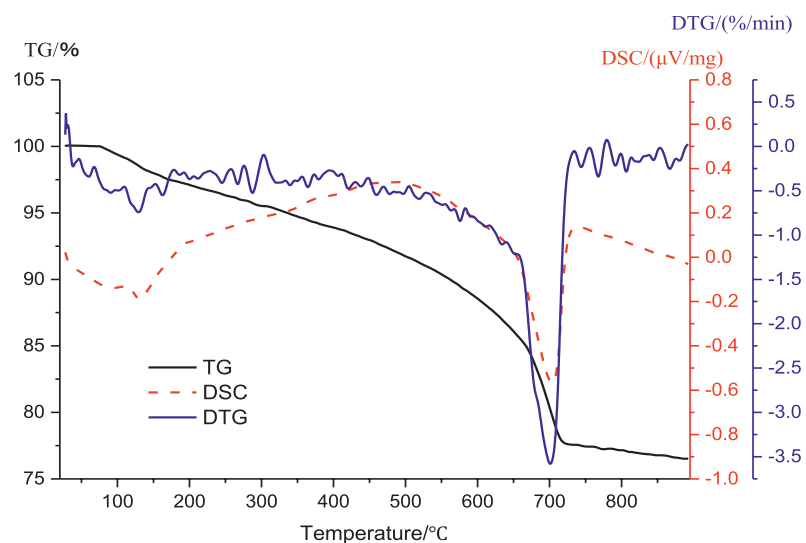


Fig. 5. TG-DSC curve of concrete powder.

Table 2. Results of house inclination measurement.

Location	Height of the house (m)	Degree of inclination (mm)	Ratio of inclination (%)	Direction
1×B	17.5	5	0.3	West
	17.5	17	1.0	South
1×E	17.5	6	0.3	West
	17.5	5	0.3	South

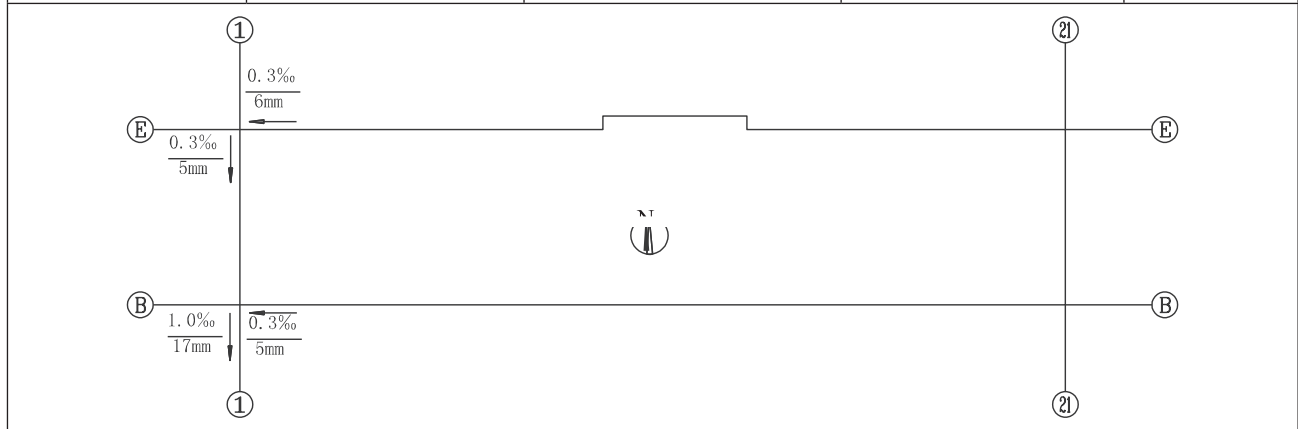


Table 3. Chemical composition of the powders of concrete in wt. %.

Ca	Si	Al	Fe	K	Na	S	Mg	Cl	Ti	Others
50.23	25.85	7.03	5.33	3.28	2.43	1.80	1.55	1.47	0.54	0.49

Table 4. Oxide composition of the powders of concrete in wt. %.

CaO	SiO ₂	Al ₂ O ₃	Fe ₂ O ₃	SO ₃	Na ₂ O	K ₂ O	MgO	Cl	TiO ₂	Others
38.23	37.75	9.45	3.52	2.80	2.41	2.31	1.86	0.90	0.42	0.35

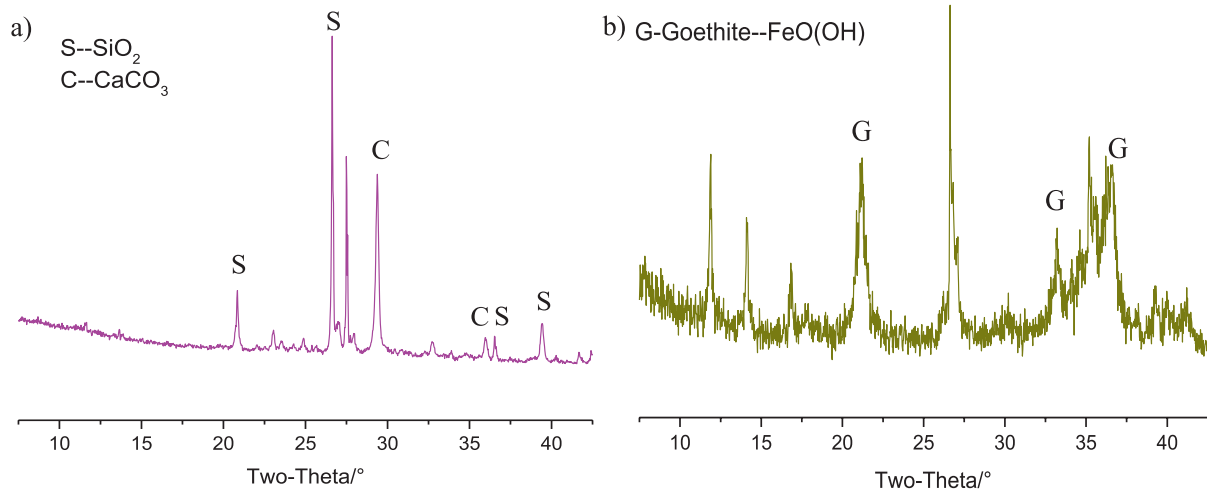


Fig. 6. XRD pattern: a) Concrete powder; and b) corrosion steel powder.

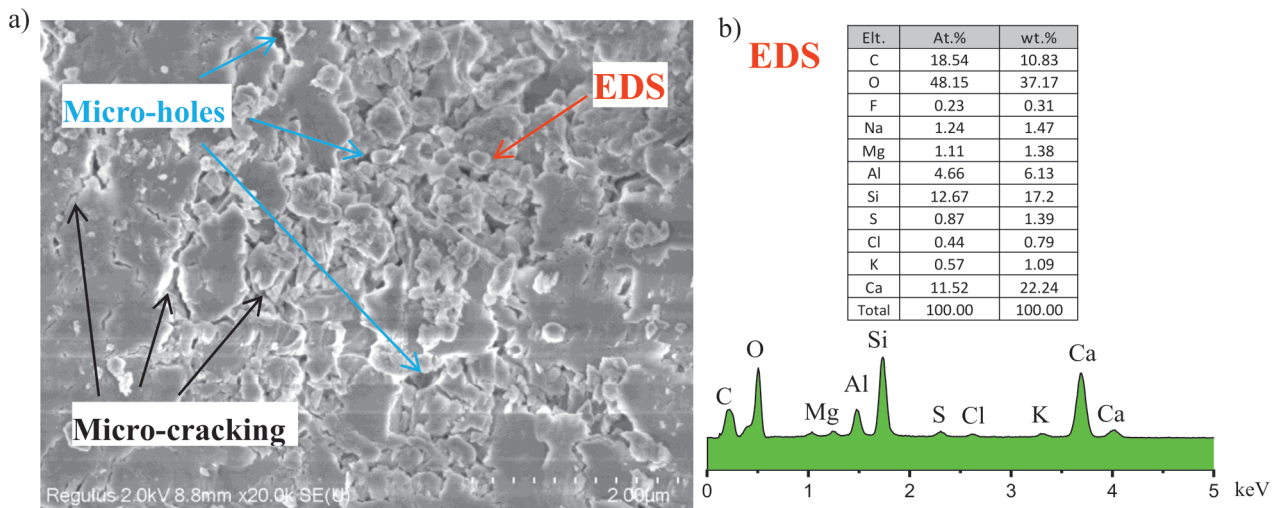


Fig. 7. a) SEM images of concrete; and b) energy spectrogram.

Check on Structural Bearing Capacity

Establishment of a Computational Model of the Structural Frame

The structural assessment of the house was conducted based on the on-site investigation, functional requirements, and load conditions. To perform the analysis, the structural calculation software PKPM, developed by the CAD Engineering Department of China Academy of Building Research, was utilized. The resulting model, obtained from the software, is shown in Fig. 8.

Establishment of a Computational Model of the Structural Frame

According to GB 50009-2012 [30], the specific dimensions of the members and construction methods, the standard load values of the house are as follows:

(1) Standard load value of floor (precast panel): dead load is 3.0 kN/m²; live load is 2.0 kN/m²; (2) standard load value of floor (cast-in-place panel): dead load is 3.5 kN/m²; live load is 2.0 kN/m²; (3) standard load value of roof (precast panel): dead load is 5.0 kN/m²; live load (overhead roof) is 0.5 kN/m²; (4) standard load value of staircase (precast terrazzo treads): dead load is 6.5 kN/m²; live load is 3.5 kN/m².

This paper was to analyze the actual compressive bearing capacity of concrete beams and columns, whose strength was designated as 19 MPa based on the on-site investigation results. The structural calculation software PKPM was used to check the bearing capacity and the results showed that the main members in several places (22 sites on the 1st floor, 8 sites on the 2nd floor and one site on the 3rd floor) failed to meet the requirements stated in Article 5.2.2 of GB 50292-2015 that the ratio of the bearing capacity of concrete structural members to its effect should reach a_u level. The details are given in Table 5. The bearing capacity of

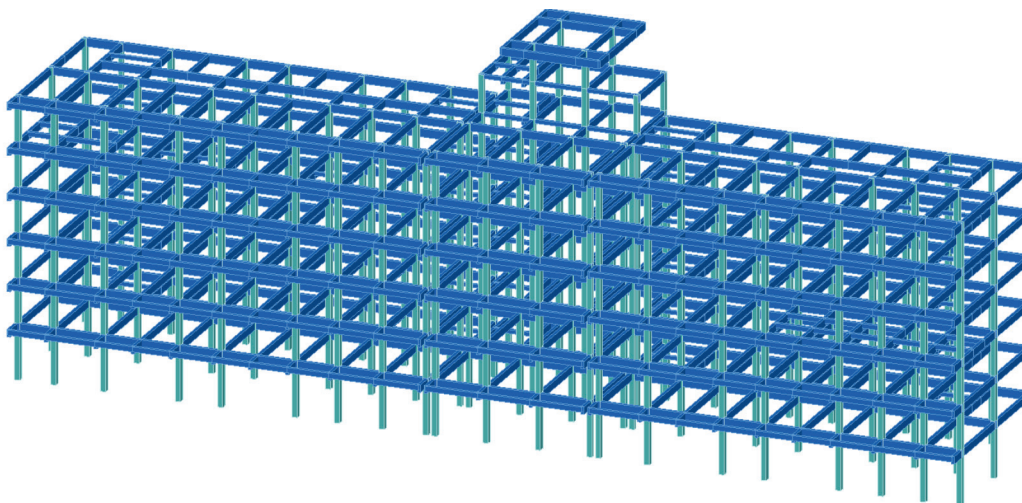


Fig. 8. Structural calculation model of the house.

Table 5. Statistical table of components that do not meet structural verification.

Number	Category	Type	Location	Check result	Class
1	Main component	Concrete column	1 st floor axis 2×C, 3×B, 3×C, 4×B, 4×C, 5×B, 5×C, 6×B, 6×C, 15×B, 15×C, 16×B, 16×C, 17×C and 18×C; 2 nd floor axis 3×C, 4×C, 5×C, 6×C, 15×C, 16×C, 17×C and 18×C	$\frac{R}{\gamma_0 S} < 0.90$	d_u
2			1 st floor axis 3×E and 18×B	$0.95 > \frac{R}{\gamma_0 S} \geq 0.90$	c_u
3			1 st floor axis 8×C, 9×C, 17×B, 19×B and 20×B; 3 rd floor axis 3×C	$1.00 > \frac{R}{\gamma_0 S} \geq 0.95$	b_u

other concrete structural members to its effect reached a_u level.

Overall Safety Assessment of the House

Foundation

The on-site investigation revealed that no settlement, deformation or cracks occurred in the house's superstructure, and the foundation was stable without differential settlement which may affect the main structure. According to Article 7.2.3 of GB 50292-2015, the safety grade of the foundation was rated A_u .

Upper Load-Bearing Structures

(1) Rating of load-bearing function of structures

According to Article 7.3.5 of GB 50292-2015, main members and their safety grades were rated below: on the first floor, there are 287 main members, of which 19 concrete columns were rated as the grade of d_u , 2 concrete columns c_u , 5 concrete columns b_u , and the other members were rated as a_u , resulting in the overall safety grade of the first floor of D_u ; on the second floor, there are 288 main members, of which 13 concrete columns were rated as d_u and the other members a_u , so the overall safety grade was D_u ; on the third floor, there are 309 main members, of which 3 concrete columns were rated as d_u , 1 concrete column b_u , and the remaining members a_u , so its overall safety grade is C_u ; on the fourth floor, there are 295 main members, of which 2 concrete columns were rated as c_u , and the rest members a_u , so the safety grade of the fourth floor was B_u ; from the fifth floor to part of the eighth floor, a total of 642 main members were rated as a_u , so their safety grades were A_u .

According to Article 7.3.6 of GB 50292-2015, common members and their safety grades were rated the following: from the 1st floor to part of the 8th floor, a total of 779 common members were rated a_u grade, so their safety grades were rated A_u .

According to Article 7.3.8 of GB 50292-2015, the safety grade of load-bearing function of the structures was rated D_u .

(2) Rating of structural integrity

The main structures of the house were constructed in accordance with the design plan. The structural layout was reasonable, and the overall system was complete. The selection of structure typology and the design of force transmission route were accurate and were conformed with national design specifications. However, reinforcement bars corroded, and concrete burst in some concrete beams and columns. According to Article 7.3.9 of GB 50292-2015, the safety grade of the structural integrity was B_u .

(3) Rating of lateral displacement of structures

The detection results showed that the maximum lateral displacement of the outer wall of the house is 25 mm, the wall is 11.2 m in height (H), and the vertex displacement is $H/448$, less than the lateral displacement limit value of $H/200$ which determines whether lateral displacement of a structure can be rated C_u or D_u , according to Article 7.3.10 of GB 50292-2015. Therefore, the safety grade of the lateral displacement of the structure was rated B_u .

According to Article 7.3.11 of GB 50292-2015, the safety grade of the upper load-bearing structures was rated D_u .

The Load-Bearing Part of the Containment System

Water seepage occurred in the outer walls, canopies and gutters of the house. The surface layer of the house was basically intact, and there were several signs of dampness at the foot of the wall. According to Article 7.4 of GB 50292-2015, the safety grade of the load-bearing part of the house containment system was rated B_u .

According to Article 9.1.2 of GB 50292-2015, the overall safety grade of the house was rated A_{su} , which was lower than the designated A_{su} grade in GB 50292-2015, thus significantly affecting the overall load-bearing capacity of the house. Therefore, effective measures must be taken immediately.

Note: A_u , B_u , C_u and D_u are the safety grades of the sub-system, and A_{su} and D_{su} are the safety grades of the appraiser system.

Conclusions

This study highlights that a reinforced concrete building, originally designed with a working life of 50 years, exhibits significant safety issues after being in service for 35 years. Therefore, we strongly recommend conducting a comprehensive investigation of buildings located in offshore areas to ensure their overall safety.

Despite minimal changes in the strength of the concrete materials, the corrosion of certain reinforcement bars within the concrete is remarkably severe. This can be attributed to the high chloride ion content in the concrete, which may be a result of using sea sand during construction or the proximity of the building to the sea. The corrosion of reinforced concrete poses safety risks to the structural members or even the entire building, necessitating special attention.

On-site inspections, which are both practical and effective for assessing the durability and predicting the service life of concrete structures, allow inspectors to examine the actual stress-bearing conditions of the buildings. This method is commonly employed for durability assessments in the present era. Additionally, microscopic analysis of the chemical composition is vital for understanding the damage mechanisms of buildings. These results help analyze the causes and mechanisms of damage while corroborating relevant macroscopic physical changes.

Durability issues can have a significant impact on the service life of concrete structures, especially in the case of offshore buildings. While durability has gained attention in the design stage of many newly constructed structures, it remains crucial to address the durability problems of in-service buildings. Since different environments and service conditions contribute to various causes of durability issues, it is essential for relevant personnel to be aware of these concerns and seek professional analysis of the causes. This will enable the development of targeted solutions to mitigate the durability problems effectively.

Conflict of Interest

The authors declare no conflict of interest.

References

1. YU H.F., DA B., MA H.Y., ZHU H.W., YU Q., YE H.M., JING X.S. Durability of concrete structures in tropical a toll environment. *Ocean Eng.* **135**, 1, **2017**.
2. GJORV O.E. Durability design of concrete structures in severe environments; China Building Materials Press: Beijing, China, **2015**; ISBN: 978-7-51601-175-1 [In Chinese].
3. YAO J.W., CHEN J.K., LU C.S. Fractal cracking patterns in concretes exposed to sulfate attack. *Materials.* **13**, 71, **2019**.
4. YAO J.W., YANG Y.Z., CHEN J.K. A novel chemo-mechanical model for fracture toughness of mortar under sulfate attack. *Theor. Appl. Fract. Mec.* **109**, 102762, **2020**.
5. CHEN J.K., JIANG M.Q., ZHU J. Damage evolution in cement mortar due to erosion of sulphate. *Corros. Sci.* **50** (9), 2478, **2008**.
6. YAO J.W., CHEN J.K., LU C.S. Entropy evolution during crack propagation in concrete under sulfate attack. *Constr. Build. Mater.* **209**, 492, **2019**.
7. XU H., CHEN J.K. Coupling effect of corrosion damage on chloride ions diffusion in cement based materials. *Constr. Build. Mater.* **243**, 118225, **2020**.
8. CHEN J.K., QIAN C., SONG H. A new chemo-mechanical model of damage in concrete under sulfate attack. *Constr. Build. Mater.* **115**, 536, **2016**.
9. WU Z.Y., YU H.F., MA H.Y., ZHANG J.H., DA B., ZHU H.W. Rebar corrosion in coral aggregate concrete: Determination of chloride threshold by LPR. *Corros. Sci.* **163**, 108238, **2020**.
10. DA B., CHEN Y., YU H.F., MA H.Y., YU B., CHEN D., CHEN X. Influence of steel corrosion on axial and eccentric compression behavior of coral aggregate concrete column. *Front. Struct. Civ. Eng.* **15**, 1415, **2021**.
11. DA B., YU H.F., MA H.Y., CHEN D., WU Z.Y., GUO J.B. Electrochemical study on steel corrosion in coral aggregate seawater concrete. *Emerg. Mater. Res.* **9**, 642, **2020**.
12. ALHAWAT M., ASHOUR A. Bond strength between corroded steel and recycled aggregate concrete incorporating nano silica. *Constr. Build. Mater.* **237**, 117441, **2020**.
13. ŠAVIJA B., LUKOVIC M. Carbonation of cement paste: Understanding, challenges, and opportunities. *Constr. Build. Mater.* **117**, 285, **2016**.
14. CARBONELL-MARQUEZ J.F., GIL-MARTIN L.M., FERNANDEZ-RUIZ M.A., HERNANDEZ-MONTES E. Procedure for the assessment of the residual capacity of corroded B-regions in RC structures. *Constr. Build. Mater.* **121**, 519, **2016**.
15. ANDRADE C. Steel corrosion rates in concrete in contact to sea water. *Cem. Concr. Res.* **165**, 107085, **2023**.
16. ANGST U., ELSENERI B., LARSEN C.K., VENNESLAND Ø. Critical chloride content in reinforced concrete-A review. *Cem. Concr. Res.* **39**, 1122, **2009**.
17. OUYANG W.Y., CHEN J.K., JIANG M.Q. Correlation analyses on physical and mechanical parameters of concrete in marine environments. *Materials* **15**, 1812, **2022**.
18. YAO J.W., CHEN J.K. Sensitivity analysis of the deterioration of concrete strength in marine environment to multiple corrosive ions. *Front. Struct. Civ. Eng.* **16**, 175, **2022**.
19. XIE N., DANG Y.D., SHI X.M. New insights into how MgCl₂ deteriorates Portland cement concrete. *Cem. Concr. Res.* **120**, 244, **2019**.
20. ALTHOEY F., FARNAM Y. The effect of using supplementary cementitious materials on damage development due to the formation of a chemical phase change in cementitious materials exposed to sodium chloride. *Constr. Build. Mater.* **210**, 685, **2019**.
21. WANG Y., NANUKUTTAN S., BAI Y., BASHEER P.A.M. Influence of combined carbonation and chloride ingress regimes on rate of ingress and redistribution of chlorides in concretes. *Constr. Build. Mater.* **140**, 173, **2017**.
22. LIU W., CUI H.Z., DONG Z.J., XING F., ZHANG H.C., LO T.Y. Carbonation of concrete made with dredged

- marine sand and its effect on chloride binding. *Constr. Build. Mater.* **120**, 1, **2016**.
23. SHEN X.H., JIANG W.Q., HOU D.S., HU Z., YANG J., LIU Q.F. Numerical study of carbonation and its effect on chloride binding in concrete. *Cem. Concr. Compos.* **104**, 103402, **2019**.
 24. DELNAVAZ A., RAMEZANIANPOUR A.A. The assessment of carbonation effect on chloride diffusion in concrete based on artificial neural network model. *Mag. Concr. Res.* **64**, 877, **2012**.
 25. JIN W.L., ZHAO Y.X. *Durability of Concrete Structures*, Science Press: Beijing, China, 58, **2002** [In Chinese].
 26. Ministry of Housing and Urban-Rural Development of the People's Republic of China. Technical Specification for Inspecting of Concrete Compressive Strength by Rebound Method JGJ/T 23-2011, China Architecture Publishing & Media Co., Ltd.: Beijing, China, **2011** [In Chinese].
 27. Ministry of Housing and Urban-Rural Development of the People's Republic of China. Code for Deformation Measurement of Building and Structure JGJ 8-2016, China Architecture Publishing & Media Co., Ltd.: Beijing, China, **2016** [In Chinese].
 28. Ministry of Housing and Urban-Rural Development of the People's Republic of China. Standard for Appraisal of Reliability of Civil Buildings GB 50292-2015, China Architecture Publishing & Media Co., Ltd.: Beijing, China, **2015** [In Chinese].
 29. Ministry of Housing and Urban-Rural Development of the People's Republic of China. Code for Design of Concrete Structure GB 50010-2010 (2015 edition), China Architecture Publishing & Media Co., Ltd.: Beijing, China, **2015** [In Chinese].
 30. Ministry of Housing and Urban-Rural Development of the People's Republic of China. Code for the Design of Building Structures GB 50009-2012, China Architecture Publishing & Media Co., Ltd.: Beijing, China, **2012** [In Chinese].